Results in Control and Optimization 14 (2024) 100389

Contents lists available at ScienceDirect

Results in Control and Optimization

journal homepage: www.elsevier.com/locate/rico

Genetic algorithm based tuning of sliding mode controllers for a boost converter of PV system using internet of things environment

Roberto Inomoto [a,b,*], Alfeu J. Sguarezi Filho [b], José Roberto Monteiro [c], Eduardo C. Marques da Costa [a]

[a] Polytechnic School of the University of São Paulo - POLI-USP, SP, Brazil
[b] Center for Engineering, Modeling and Applied Social Sciences, Federal University of ABC - UFABC, SP, Brazil
[c] School of Engineering of São Carlos, University of São Paulo, SP, Brazil

ARTICLE INFO

Keywords:
Photovoltaic
Boost converter
Maximum power point tracking
Genetic algorithm
Sliding mode control

ABSTRACT

This paper proposes a novel controller optimization of boost converter by tunning two controllers of voltage and current in PV (Photovoltaic) boost converters: Sliding Mode Control (SMC) or Sliding Mode plus Proportional-Integrative. Genetic Algorithm (GA) optimization is applied in a Internet of Things (IoT) context, in which the server side consists of running the GA and thereafter used to tune the SMC and SMPIC of the PV plant boost converter. Communication between the IoT (PV plant) and cloud server comprises to the acquired currents and voltages from PV to the server and controllers parameters from server to IoT. Data from the IoT is applied to calculate the fitness function for a given solution, which learns the solar plant (machine learning). Experimental results using hardware are considered, in order to evaluate the performance, and results are compared between heuristic and deterministic parameters from SMC or SMPIC, proving the reduction of overshoot and settling time.

1. Introduction

PV power generation is directly influenced by environmental conditions, such as: solar irradiation and temperature of the modules. In this sense, the optimization of the PV system power generation requires an algorithm that leads to the maximum power point of the PV module (solar panel), such as the so called *Maximum Power Point Tracking* - MPPT [1]. However, the optimization of the MPPT can be obtained from the investigation on the transient response of the controllers, i.e. the controllers ability to regulate and maintain a given output based on a reference value and to respond to sudden changes. Some linear controllers are found in the technical literature, such as: the proportional–integral (PI), lead-leg [2] or the state feedback controllers [3]. In addition, there are also the nonlinear controllers, i.e. the PV module has a nonlinear behavior of voltage-current curve, which is highly dependent on the environmental conditions and technical issues. The nonlinear controllers are widely associated with other control techniques, such as: Fuzzy Logic controller [4], nonlinear-adaptive controllers [5], adaptive controllers [6], finite control set model predictive control [7,8], neural network [9] and sliding mode controllers (SMC) [10].

In PV power generation applications, the SMC shows a notable advantage over other nonlinear controllers: a simplified mathematical development and application. In addition, the SMC has been proposed in association with other well-established techniques: smooth switching function; higher order sliding surface (HOSS), which has an integral component. Such techniques prove to be robust and accurate in simulations as well as on bench [11].

* Corresponding author at: Polytechnic School of the University of São Paulo - POLI-USP, SP, Brazil.
E-mail addresses: roberto.inomoto@usp.br (R. Inomoto), jrm@sc.usp.br (J.R. Monteiro), educosta@usp.br (E.C.M. da Costa).

https://doi.org/10.1016/j.rico.2024.100389
Received 28 October 2023; Received in revised form 16 December 2023; Accepted 2 February 2024
Available online 5 February 2024
2666-7207/© 2024 The Authors. Published by Elsevier B.V. This is an open access article under the CC BY-NC-ND license (http://creativecommons.org/licenses/by-nc-nd/4.0/).

The study of optimization methods are presented on the premise of finding the best possible result for the proposed controller. The optimization methods seek to find the values of the parameters that minimize the objective function while complying with some restrictions [12], being a powerful tool for controller design. GA is an adaptive heuristic search-based optimization technique were originally developed by John Holland in 1960 [13]. GA is a natural selection inspired algorithm which is based on the concepts of Darwinian evolution. It is frequently used to solve optimization problems in research and machine learning solutions for difficult problems which would take a lifetime to solve it [14].

In [15], a GA is implemented to determine the parameters for the neural network based PID (Proportional–Integral Derivative) controller and the results are compared with and without using optimization for a boost converter. The new GA searched parameter plant was computationally simulated and it was observed an overshoot reduction and an improved settling time over the original controller, i.e., without parameter optimization. In [16] the same study was made for a buck converter.

Another type of optimization method applied to a boost converter in PV system is implemented in [10]: A Weighted-Particle Swarm Optimization (w-PSO) applied to tune Sliding Mode plus PI controller. Firstly, it was mathematically modeled using AC small signal technique and the Slide Mode Control law was defined. Then, w-PSO was used to obtain the optimal parameters thorough computational simulation and carried out in a boost converter prototype.

However, most of optimization ran in simulation before carrying over real prototype, which has the following issues: rounds, approximation and constraints. How about take advantage over network to monitor, data logging or even optimize the solar plant?

IoT is an interconnected network of objects which devices could be a simple sensor to a smart device [17]. IoT is growing so fast nowadays and it is possible to take advantage over networking usage focused in solar plant. IoT is the core of the modern electronic devices through the benefit of plant automation and control. This benefit can take advantage of the wealth of information that can generate on the plant but also in other areas like process, industrial, and machinery [18]. This technology can provide for the plant new set of tools and information to further optimize the plant. This kind of information integrates the plant and its real-time data, diagnostics through telemetry. It can reduce operational cost, increase lifetime, and performance customization. The information is exchanged between devices for data logging, monitoring and decision making to create an autonomous mesh of intelligent assets via wired or wireless transmission.

In this context, work [19] presents a PV system IoT-based using an Arduino and ESP to monitor and provide online the PV current, PV voltage, load voltage, load current and duty-cycle. It is implemented the most common tracking algorithms and shown the results. As this is a low cost project, the results are stable but the performance are not satisfactory. Works [20,21], and [22] have similar approach as [19], which monitor voltage and current.

An improvement of voltage profiles at different load nodes and reduce power losses in transmission lines presented in work [23]. An optimization algorithm is responsible for finding out the optimal reactive power setpoint for each plant in real time based on an IoT solution which requires the transmitted data and using the system mathematical model. An improvement up to 68% in the global voltage profiles in the load buses has achieved.

In this way, the proposal of this paper is an adaptive heuristic search algorithm finding parameters for the controllers proposed by the same authors in SMC [11] and SMPIC [10]. The mathematical model of these two controllers are consolidated in the area and are detailed in the aforementioned articles. In other works [2,10,15,16], heuristic search runs in simulation and then are applied the prototype. And, the mentioned solution is not employed in this proposal. This work uses the benefit of IoT concept to find the parameters of the controllers in runtime, which are evaluated by GA directly in the cloud server from data received using internet connection. Data are obtained from tests performed on the prototype with real components. Hence, the modeling approximation errors are removed, system can run with optimized controller already found and it is possible to achieve some improvements in the system performance.

This paper is structured as follows. The proposed sliding mode control are shown in Section 2. The GA description is presented in Section 3. Results using hardware are given in Section 4. Finally, conclusion are presented in Section 5.

2. Topology

This Section discusses the PV system, which is compounded by a PV panel connected to a boost converter which is controlled by SMC [11] or SMPIC [10] and an inverter which converts direct current to alternating current (DC/AC). And the networking infrastructure which the PV system connects to a cloud server running the GA to monitor and eventually reconfigure the controller over ethernet. The topology is shown in Fig. 1.

2.1. Boost converter

Boost converter increases and regulates the PV panel voltage v_{PV} to a level needed by a system connected on its output (V_{DC}), for example, an inverter, depending on the application, as shown in Fig. 1.

The input voltage (v_{PV}) and inductor current (i_L) of boost converter are controlled through a constant switching frequency (Pulse-Width Modulation - PWM_{Boost}) signal to switch on or off the MOSFET (Q_{SW}). The block diagram shows the controller divided in two loops: The MPPT algorithm provides the reference voltage (v_{PVref}) to the outer voltage control loop. This stage regulates the DC component of v_{PV} to its set point, giving an inductor current reference (i_{Lref}) to the inner current control loop. The inner current control loop calculates the i_L and generates a duty cycle (d) through a PWM_{Boost} for Q_{SW}

When the Q_{SW} is switched on, the output stage is isolated due the diode (D) is reversed biased. The inductor (L) is connected to the ground and the current flows through it, storing energy [24]. When Q_{SW} is switched off, the energy from L, plus the energy from the input capacitor (C_{PV}) flows through D to V_{DC}. The output capacitor (C_O) is assumed to be quite large to ensure a constant output voltage [25].

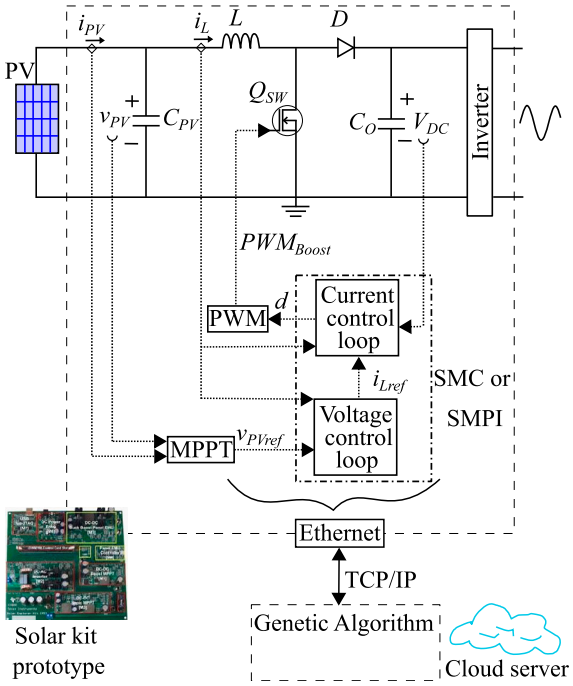

Fig. 1. Block diagram of PV system.

2.2. Mathematical model

A method to linearize the PV module at a straight line tangent to its I-V curve at the operation point obtains a linear equivalent model of the circuit [26].

The dynamic equations corresponding to the state of the circuit when Q_{SW} is closed are obtained by evaluating the derivatives of the inductor current and capacitor voltage:

$$\begin{cases} \dfrac{di_L}{dt} = \dfrac{v_{PV}(t)}{L} \\ \dfrac{dv_{PV}(t)}{dt} = \dfrac{V_{eq} - v_{PV}(t)}{R_{eq}C_{PV}} - \dfrac{i_L(t)}{C_{PV}}, \end{cases} \tag{1}$$

where V_{eq} is a linearization of PV panel voltage and R_{eq} is a linearization of PV panel resistance [27].

The dynamic equations when Q_{SW} is opened are given by:

$$\begin{cases} \dfrac{di_L(t)}{dt} = \dfrac{v_{PV}(t) - V_{DC}}{L} \\ \dfrac{dv_{PV}(t)}{dt} = \dfrac{V_{eq} - v_{PV}(t)}{R_{eq}C_{PV}} - \dfrac{i_L(t)}{C_{PV}}. \end{cases} \tag{2}$$

2.3. Sliding Mode Plus PI Control (SMPIC)

The control objectives for the system are related to the error between the measured variable and the reference, since the control scheme aims to reduce the error to zero. The sliding surface is defined through the voltage error and the current error.

However, to increase the dynamic response of the controller, the errors (e_v and e_i) derivatives are added, obtaining two second order sliding surfaces:

$$\sigma = \begin{bmatrix} \sigma_1 \\ \sigma_2 \end{bmatrix} = \begin{bmatrix} e_v + k_v \dfrac{de_v}{dt} \\ e_i + k_i \dfrac{de_i}{dt} \end{bmatrix} = 0, \tag{3}$$

where the constants k_v and k_i are defined according to the desired dynamics.

The sliding variable σ is switched through the $S(x)$ function, which is also responsible for determining the reaction of the system to changes in the state variables. The $S(x)$ function operates by limiting the surface when it reaches one of its maximum or minimum

values and also, due to its linear nature, it is sensitive to the reduction of the chattering when the state approximates the switching surface [28], as defined by:

$$S(x) = \begin{cases} 1 & \text{if } x > 1 \\ x & \text{if } -1 \leq x \leq 1 \\ -1 & \text{if } x < -1 \, . \end{cases} \tag{4}$$

The control laws for both control loops are defined as [10]:

$$i_{Lref} = (k_{pv} + \frac{k_{iv}}{s}) S(\sigma_1) \tag{5}$$

and

$$d = (k_{pc} + \frac{k_{ic}}{s}) S(\sigma_2), \tag{6}$$

where k_{pv}, k_{iv}, k_{pc}, and k_{ic} are gains of PI controller.

2.4. Sliding Mode Control (SMC)

2.4.1. Current control loop

Considering a First Order Sliding Mode Control and a First Order Sliding Surface, the (1) and (2) could be written:

$$\frac{di_L(t)}{dt} = \frac{1}{L} \frac{2v_{PV}(t) - V_{DC}}{2} + \frac{1}{L} \frac{V_{DC}}{2} \text{sign}(\sigma_I), \tag{7}$$

where $\sigma_I = i_{Lref} - i_L$.

In order to improve dynamic response, mainly for eliminate steady state error due to the use of the soft switching function (4), an integrative second order sliding surface can be adopted [29]:

$$\sigma_i = \int \lambda(e_i) e_i dt + e_i = 0, \tag{8}$$

where σ_i is the sliding variable, $e_i = i_{Lref} - i_L$ and $\lambda(e_i)$ is a function that must satisfy the attractiveness condition for the system, as described in [11]. Thus, the current controller is:

$$d = \frac{S(k_i \sigma_i) + 1}{2}, \tag{9}$$

where $k_i > 0$ and can be arbitrarily chosen as a compromise between chattering and speed response.

2.4.2. Voltage control loop

For the voltage control loop an integrative second order sliding surface is also chosen:

$$\sigma_v = \int \lambda(e_v) e_v dt + e_v = 0, \tag{10}$$

where σ_v is the sliding variable, $e_v = v_{PVref} - v_{PV}$ and $\lambda(e_v)$ is a function that must satisfy the attractiveness condition for the system.

Then, the voltage loop controller is:

$$i_{Lref} = I_{MAX} \frac{1 - S(k_v \sigma_v)}{2}, \tag{11}$$

where I_{MAX} is the maximum current value allowed for the components and k_v is the same as k_i for (9), the coefficient of the smooth switching function.

3. Genetic Algorithm - GA

The reliable hardware and software technique evolution is capable to monitor, reconfigure and detect fault in any system. This technique can be named as machine or deep learning. GA, IoT and big data analytics (BDA) have seen development to automate plants. These technologies aim to develop innovative, autonomous, and smart condition-monitoring concepts for precise failure detection and classification as well as intelligent decision making for rapid actions in plants [30].

In this Chapter, it is discussed the GA implementation in the cloud server, which the proposed research, the flowchart of GA is depicted in Fig. 2. GA starts with an initial given problem and then, plant is evaluated in runtime and assigned for a fitness function, which gives a chance for possible solution. Otherwise, if not satisfied, this population goes for a recombination and mutation, as in natural genetics, producing new children, and the process is repeated over various generation. Hence, it keeps evolving better individuals by every generation until reach the criterion [31]. The proposed GA runs on IoT system composed by cloud server and real solar plant prototype. The cloud server exchange data through network sending to the real plant the SMC/SMPIC parameters and cloud server receives the current and voltage acquisition instantaneously. It is important to mention that the solar plant prototype has the overvoltage and overcurrent protections necessary to guarantee the system operation.

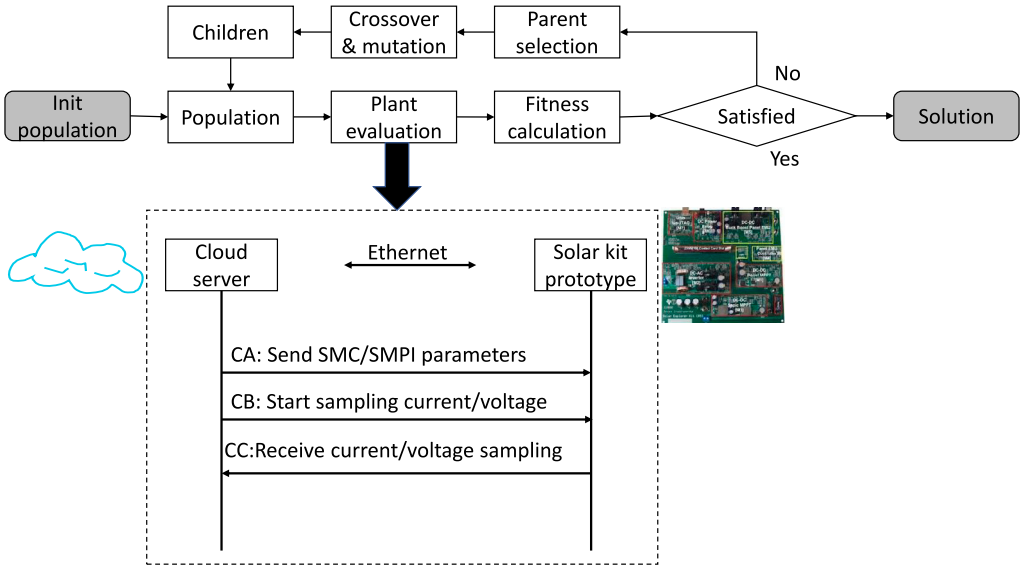

Fig. 2. GA algorithm.

3.1. Initial population

The population is initialized with N random parents which represents the possible candidate solution. A chromosome is one solution for the given problem and gene is one element position of a chromosome.

3.2. Fitness function

Once the initial population is created, it is determined the performance of each individual using an adaptive function, which assigns to each possible solution a fitness function that reflects its quality [14]. For the proposed topology, the quality criteria are overshoot and settling time which this definition is very important task because the GA uses the information to choose the best solution in the final population.

Since there are two controllers for the proposed PV system topology, for the current control loop and voltage control loop the fitness function is defined by:

$$ITAE = \int_0^{\tau} t|e(t)|\,dt \tag{12}$$

and

$$ISE = \int_0^{\tau} e^2(t)\,dt, \tag{13}$$

where the first is (useful) to reduce the contribution of error that remains over time and the second is useful to reduce large errors. It is expected for the PV system a small overshoot and low steady-state oscillation using these 2 equations [10]. So, while running the optimization process for both controllers, smaller result is better.

3.3. Parent selection

Parent selection is a process to choose parents for recombination and create an offspring for next generation. A good amount of parents diversity is a very important item to not have a premature convergence. Some well used technique are Proportionate Roulette Wheel Selection, Linear Ranking Selection, Exponential Rank Selection, Tournament Selection. This last technique is more efficient in convergence and simple to implement, and low vulnerability to takeover by dominant individuals according to work [31,32]. Nonetheless, this work compared tournament selection and Proportionate Roulette Wheel Selection which was preferred to use this last one because it found faster the optimal solution.

Proportionate Roulette Wheel Selection gives higher weight for chromosomes in the population according to their fitness value and a virtual roulette wheel is "spinned" to select one of the parents [33]. The spinned roulette wheel representation is given by Eq. (14) Smaller fitness value is better, higher weight is set for those parents.

$$\text{parent} = \text{randsample}(W_1, ..W_n), \sum_{i=1}^{n} W_i = 1 \tag{14}$$

where randsample is a random number representing the roulette wheel, W_i is the ith weight.

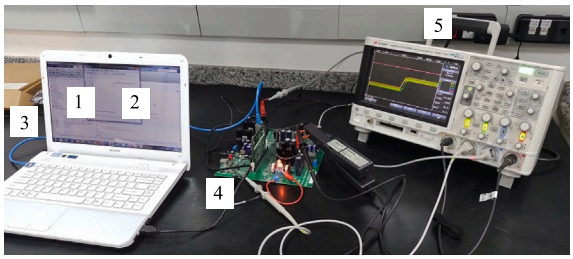

Fig. 3. Experimental bench setup. (1) Code Composer Studio (CCS); (2) Matlab; (3) Ethernet cable; (4) Solar Explorer Kit (TMDSSOLARCEXPKIT); (5) Oscilloscope.

Table 1
Operating point at maximum power of the TMDSSOLARCEXPKIT [36].

Irradiance (W/m^2)	P_{max} (W)	V_{PV_MPPT} (V)	I_{PV_MPPT} (A)
1000	36.02	18.46	1.951
900	32.42	16.42	1.975
800	28.82	14.68	1.963
700	25.22	12.77	1.975
600	21.61	10.98	1.969
500	18.01	9.093	1.98
400	14.41	7.363	1.957
300	10.81	5.473	1.975
200	7.205	3.67	1.963

Table 2
Values used for Booster converter.

Component	Value
Inductor (L)	100 μH
Capacitor (C_{PV})	680 μH
Resistor (R_{eq})	0.1986 Ω
(V_{DC}) Voltage	30 V
PWM_{boost}	100 kHz
Voltage and current sampling time	20 μs

3.4. Crossover and mutation

Crossover is a genetic operator that mix information from the selected parents to reproduce offspring for the new generation, having better child from the parents [14]. The mathematical representation of parents and children are floating-point numbers. So, for GA naming convention the chromosome representation of the proposed work is an IEEE 754 single-precision binary floating-point format [34] by Eq. (15). Floating-point number is converted in 32 gene (bit) of chromosome and random selected each gene from both parents, mixing its information, generating a new chromosome. Eventually, a mutation happens in one of the 32 gene flipping the gene value (16). Mutation is used to guarantee diversity of population, in other words, it tries to avoid local optimum and searches for global optimum solution [35]. After mutation, the 32-bit chromosome returns again to floating-point number:

$$\text{float} = s.2^{(128-e)}.m\,, \tag{15}$$

$$\text{mutation} = \text{bit}_p.q\,, \tag{16}$$

where s is sign; e is exponent; m is mantissa; p is a random number $\in \mathbb{N} = \{0, .., 31\}$; q is a random number $\in \mathbb{N} = \{0, 1\}$.

4. Hardware experimental verification

The propose of this work is to show the viability of IoT usage concept for machine learning using GA in order to optimize the SMC or SMPIC solar plant controllers. IoT has several advantages, like automate and monitoring power delivered by the solar plant or even diagnostic the system.

Texas Instrument Solar Explorer Kit (TMDSSOLARCEXPKIT) with Digital Signal Processor (DSP) F28M35H52C is employed [36]. This solar explorer kit provides a low voltage platform composed by a PV module/array emulator (laboratory usage [37]), a buck-boost converter, boost converter, a full bridge single phase-inverter, and Ethernet connection as shown in Fig. 3.

The boost converter input is supplied by the PV emulator which has a nonlinear I-V curve of PV module under different levels of irradiance, according to Table 1. The output boost capacitor and single-phase inverter maintains boost converter output voltage around 30 V. Table 2 shows the boost converter characteristics.

Table 3
Custom application commands.

Commands	Description
C2	Start PV panel emulator
C3	Stop PV panel emulator
C4	Instantaneous PV power
C5	Theoretical PV power
C6	One acquisition v_{PV}
C7	One acquisition i_L
C8	One acquisition V_{DC}
C9	Irradiance value
CA	Adjust SMC/SMPIC parameters
CB	Start acquisition of i_{Lref}, and i_L, or v_{PV}, and v_{PVref}
CC	First buffer acquisition defined by command 0xCB
CD	Second buffer acquisition defined by command 0xCB

The DSP is programmed in the C language using Texas Instrument environment called Code Composer Studio which generates binary file and can download it through an USB cable. The DSP has dual-core which one processor is designed for real-time control purpose and the ARM Cortex M3 processor is designed for communication purpose, including Ethernet connection. The real-time control core is programmed to control power electronic as the boost converter and inverter. The control logic has been explored in Section 2.2.

4.1. IoT

As discussed in previous Section, the IoT is developed in ARM Cortex M3 processor. This processor has 2 important peripherals which IoT is possible: Ethernet peripheral and Inter Processor Communication peripheral which exchange data between M3 and real-time control processor (DSP). Software implementation of the OSI (Open Systems Interconnection) model is necessary. The Network Access & Physical layer is provided by ARM processor and external hardware. The others layers are implemented in software. The Internet layer, source and destination hosts identified by IP addresses. Transport layer is implemented in TCP protocol and Application layer are implemented in HTTP and custom application commands shown in Table 3.

4.2. GA

The objective of GA is seeking for optimal parameters for SMC and SMPIC. For SMC, the parameters found in (8) and (9) for current control loop and (10) and (11) for voltage control loop. For SMPIC, the parameters found in (6) for current control loop and (5) for voltage control loop, as well as the parameters of (6) for both voltage and current control loops (Section 2). Previous SMC work [11] found the parameters by mathematical modeling and SMPIC work [10] found parameters by heuristics algorithm PSO running on simulation and uploaded to the prototype. The boost converter has some characteristics which were not considered like component tolerances, component temperature, rounds, and constraints. GA will guarantee best optimal results running in the real prototype.

GA is programmed in Matlab programming language using technique shown in Section 3. Some constraint are defined: maximum iteration is 100; size of population is always 10; fitness function defined as 20 ms and 1 ms settling time respectively for voltage and current and 10% maximum overshoot during step test.

GA runs in a cloud server and an initial random population (parameters) is created and transmitted through network (commands defined in Table 3) and these parameters are loaded into SMPIC or SMC in real boost converter prototype. DSP acquires the voltages/currents and send back to the server every 1 s to GA analyze the quality of voltages and currents using the fitness function constraints aforementioned (Plant evaluation), which is viewed in Fig. 2. Several iterations are needed to find an optimal solution.

This kind of setup have some disadvantages: it takes more time than simulation to find an optimum value; undesired bad chromosomes (which is expected in GA) could cause some spikes during plant evaluation; limited population and iteration due to the time of running the GA; processor must be powerful to run control and also support TCP/IP connection. Due to these facts, the system has to be divided into two modes of operation: normal and optimization mode.

Normal mode is the regular PV system usage, it is designed to monitor current, voltage and power, as well as controlling both control loops and MPPT algorithm. In this operation, no parameter is changed to avoid any transient and loss of performance.

Optimization mode, the designed software has the ability to exchange data between server and reconfigure SMC or SMPIC through custom commands. The optimization process is very slow to find the best performance. So, when communication link fails while in optimization mode, system returns back to normal mode using latest best parameters found.

The objective of this first experiment has to determine optimal parameters for current control loop. After ran GA in optimization mode, it has measured inductor current in normal mode, which have tracked the current reference as shown in Figs. 4(a) and 4(b), respectively before and after SMPIC parameter adjustment, when a step reference from 1.0 to 2.0 A is applied to verify the current response. These data are better shown in Fig. 4(c) which has acquired by network showing the comparison between w-PSO and GA SMPIC parameters. Same test are depicted in Figs. 5(a) and 5(b), respectively before and after GA adjustment, and Fig. 5(c) has acquired by network showing the comparison between heuristic and deterministic SMC parameters. In all those cases they have similar results as shown in Table 4. Hence, it can be observed the satisfactory performance of the GA tunning regarding steady state and settling time parameters.

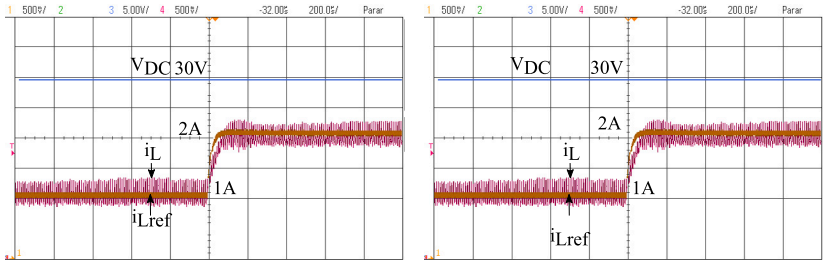

(a) w-PSO current loop SMPIC in detail measured on solar explorer kit prototype. (b) GA adjusted current loop SMPIC measured on solar explorer kit prototype.

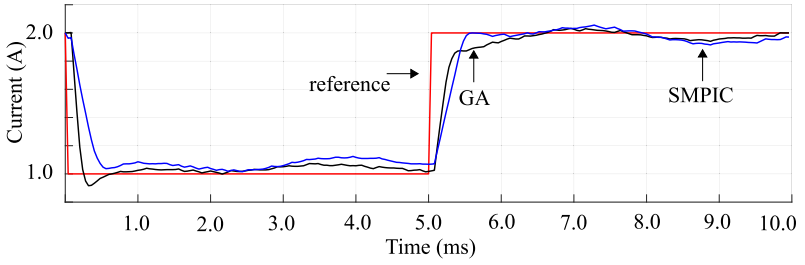

(c) Current loop comparison acquired through network on solar explorer kit prototype: (SMPIC) w-PSO SMPIC; (GA) Heuristic SMPIC.

Fig. 4. Current loop measured on bench.

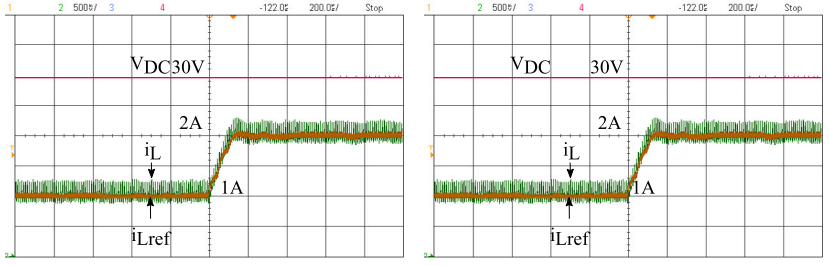

(a) Deterministic current control loop SMC measured on solar explorer kit prototype. (b) GA adjusted current loop SMC measured on solar explorer kit prototype.

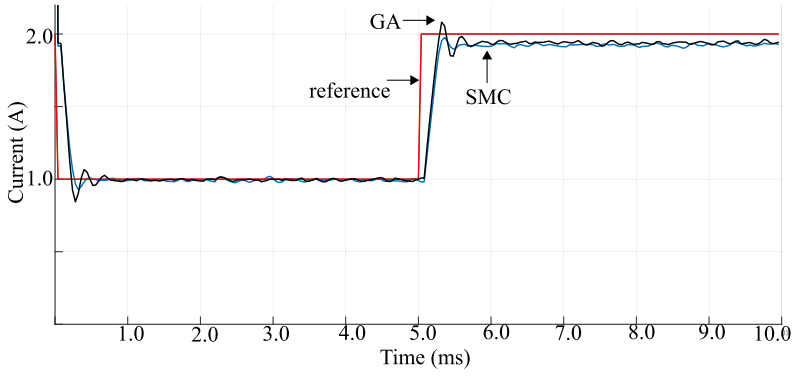

(c) Current control loop comparison acquired through network on solar explorer kit prototype: (SMC) Deterministic SMC; (GA) Heuristic SMC.

Fig. 5. Current control loop measured on bench.

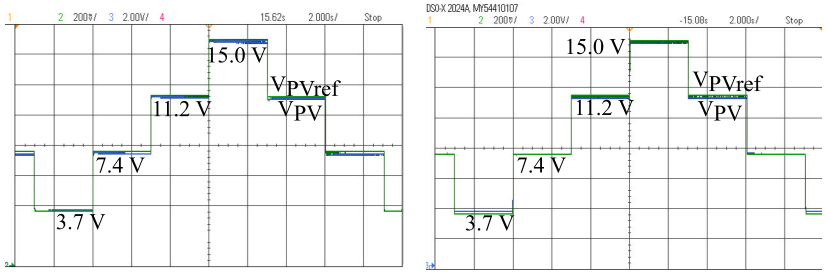

(a) GA voltage control loop SMPIC. (b) GA voltage control loop SMC.

Fig. 6. Voltage control loop measured on bench.

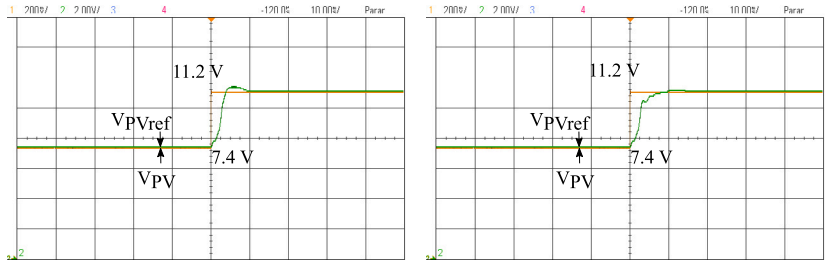

(a) GA adjusted voltage loop SMPIC step response. (b) Voltage loop SMPIC step response.

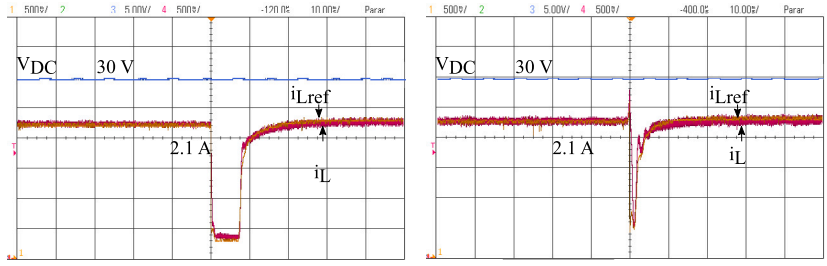

(c) Current behavior for GA adjusted voltage loop step. (d) Current behavior for voltage loop step.

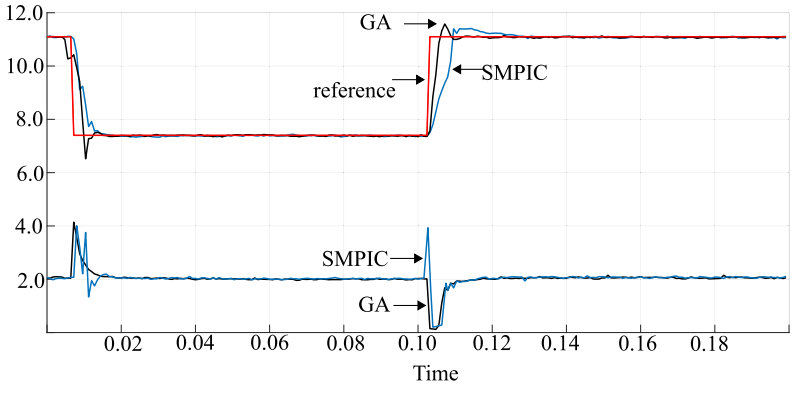

(e) Voltage loop compare and current acquired through network on solar explorer kit prototype: (SMPIC) Deterministic SMPIC; (GA) Heuristic SMPIC.

Fig. 7. Voltage loop step test measured on solar explorer kit prototype. Irradiance from 400 W/m^2 to 600 W/m^2.

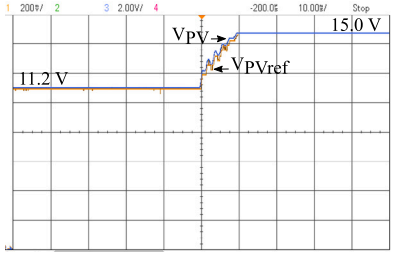

(a) GA adjusted voltage loop SMPIC step response.

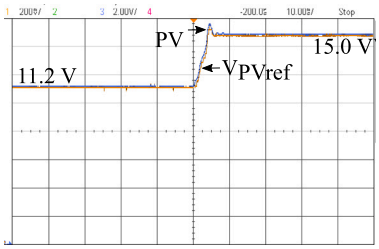

(b) Voltage loop SMPIC step response.

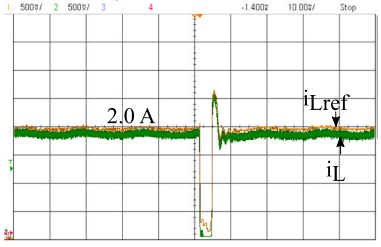

(c) Current behavior for GA adjusted voltage loop step.

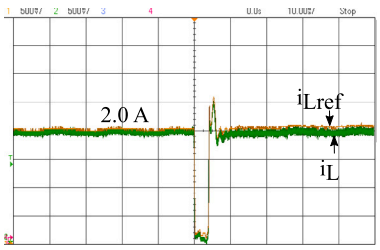

(d) Current behavior for voltage loop step.

Fig. 8. Voltage loop step test measured on solar explorer kit prototype. Irradiance from 600 W/m^2 to 800 W/m^2.

Table 4
Current step test comparison.

	SMPIC		SMC	
	w-PSO	GA	Deterministic	GA
Settling time	1 ms	1 ms	0.41 ms	0.4 ms
Overshoot	0%	0%	0%	1.1%
Steady-state error	5.1%	2.6%	2.5%	2.4%

4.3. Current control loop performance comparison

The objective of this first experiment has to determine optimal parameters for current control loop. After ran GA in optimization mode, it has measured inductor current in normal mode, which have tracked the current reference as shown in Figs. 4(a) and 4(b), respectively before and after SMPIC parameter adjustment, when a step reference from 1.0 to 2.0 A is applied to verify the current response. These data are better shown in Fig. 4(c) which has acquired by network showing the comparison between w-PSO and GA SMPIC parameters. Same test are depicted in Figs. 5(a) and 5(b), respectively before and after GA adjustment, and Fig. 5(c) has acquired by network showing the comparison between heuristic and deterministic SMC parameters. In all those cases they have similar results as shown in Table 4. Hence, it can be observed the satisfactory performance of the GA tunning regarding steady state and settling time parameters.

4.4. Performance voltage control loop comparison

Once the inner control loop are assessed, the next step comprises the evaluation of the parameters of outer voltage control employing GA, which comprises the inner current control loop. Figs. 6(a) and 6(b), respectively, for SMPIC and SMC, show 4 voltage levels tests of reference (3.7 V, 7.4 V, 11.2 V, and 15.0 V) in which it has null steady state error.

The test for a voltage step using SMPIC have measured on bench are presented in Figs. 7(a)–7(d) from 400 W/m^2 to 600 W/m^2 and Figs. 8(a)–8(d) from 600 W/m^2 to 800 W/m^2 before and after parameters adjustment. And, in the same way for the SMC, the same tests are depicted in Figs. 9(a), 9(b), 9(c), 9(d) and 10(a), 10(b), 10(c), 10(d). Those data are better presented in Figs. 7(e) and 9(e), which a step voltage reference varies from two levels: 7.4 V, 11.2 V and also 11.2 V to 15.0 V. It can be observed that the proposed optimization have better performance than w-PSO SMPIC or deterministic SMC because of their overshoot or settling time as presented in Table 5. Additionally, the current behavior for both tests have low overshoot when it employs the GA optimization.

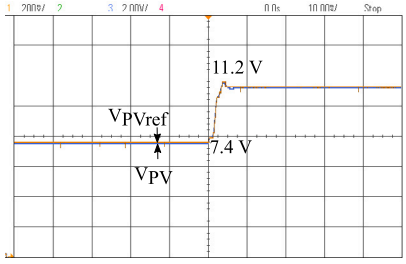

(a) GA adjusted voltage loop SMC step response.

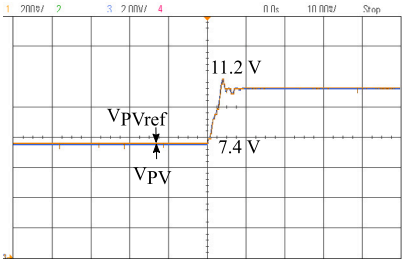

(b) Voltage loop SMC step response.

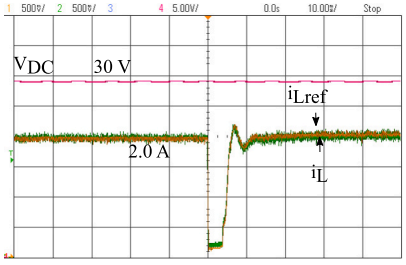

(c) Current behavior for GA adjusted voltage loop step.

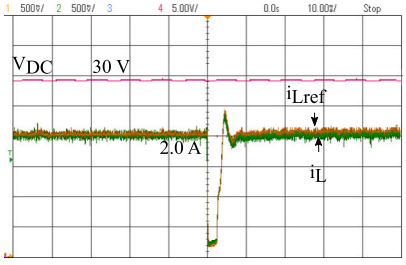

(d) Current behavior for voltage loop step.

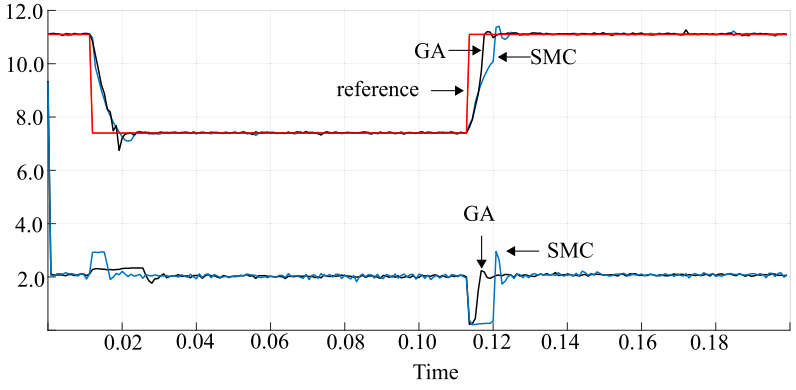

(e) Voltage loop compare and current acquired through network on solar explorer kit prototype: (SMC) Deterministic SMC; (GA) Heuristic SMC.

Fig. 9. Voltage loop step test measured on solar explorer kit prototype. Irradiance from 400 W/m^2 to 600 W/m^2.

Table 5
Voltage step test comparison.

Voltage		SMPIC		SMC	
		w-PSO	GA	Deterministic	GA
7.4 to 11.2 V	Settling time	16 ms	9 ms	10 ms	7 ms
	Overshoot	4.6%	5.4%	1.8%	0.9%
	Steady-state error	0%	0%	0%	0%
11.2 to 15.0 V	Settling time	9 ms	9 ms	10 ms	6 ms
	Overshoot	2.7%	0.1%	2.7%	1.3%
	Steady-state error	0%	0%	0%	0%

4.5. MPPT algorithm

Once the control loops are verified, the next test consists of analyzing the new SMPIC and SMC parameters performance in the presence of a step irradiation profile. Figs. 11 and 12 presents the PV control system under irradiance variations. Irradiance levels from 200 until 800 W/m^2 are tested, attesting the functionality of the controller under normal operating conditions. The values

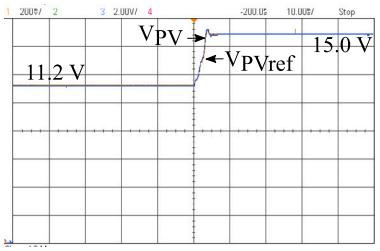

(a) GA adjusted voltage loop SMC step response.

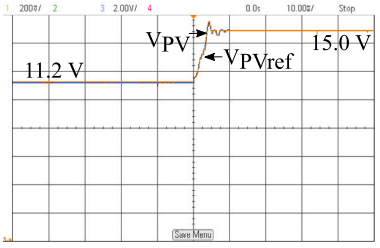

(b) Voltage loop SMC step response.

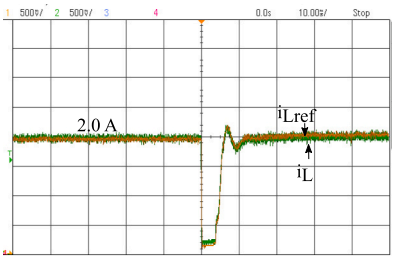

(c) Current behavior for GA adjusted voltage loop step.

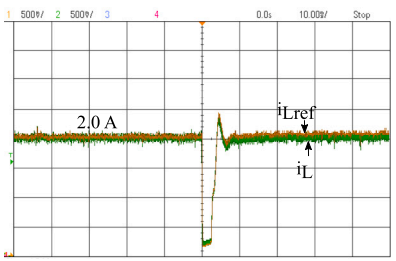

(d) Current behavior for voltage loop step.

Fig. 10. Voltage loop step test measured on solar explorer kit prototype. Irradiance from 600 W/m^2 to 800 W/m^2.

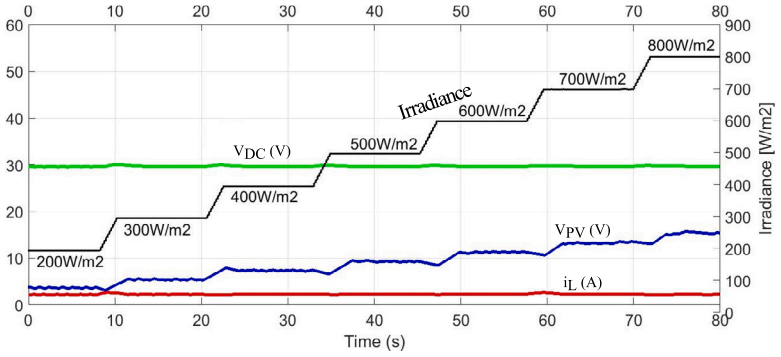

Fig. 11. Irradiation variation test for SMC.

observed in Figs. 11 and 12 are in agreement with the data presented in Table 1. In this test, the voltage reference is calculated using the incremental conductance MPPT [36]. The attained results present that the v_{PV} tracks the v_{PVref}, while the i_L current also tracks the reference i_{Lref} and the output voltage of the boost converter remains around 30 V.

On the other hand, Figs. 13 and 14, respectively for SMC and SMPI show an irradiance changing from 200 until 800 W/m^2 and goes back immediately to 200 W/m^2, which shows a very good stability. In each irradiance step, a small irradiance change is applied to the system, simulating a fast PV shading, which V_{PV} tracks V_{PVref}.

5. Conclusions

This paper has proposed a continuation of work [10,11] which they were presented respectively a SMPIC and SMC applied for a boost converter in a PV system using a constant switching frequency operation. In those previous works, for both cases, experimental tests compared the performances of SMPIC or SMC which presented better performance than lead–lag controller. So, no further comments on the best performance of these two controllers.

Normally, most of works run GA in simulation like Matlab before using these parameters on real plants, which have some disadvantages like component tolerances, mainly caused by temperature changes. Moreover, while modeling the SMPIC or SMC, linearization, approximations, constraints, and assumptions are assumed which can decrease performance. In the present work, the novelty is increasing the SMC and SMPIC performance using GA in an actual converter on bench using IoT environment, so

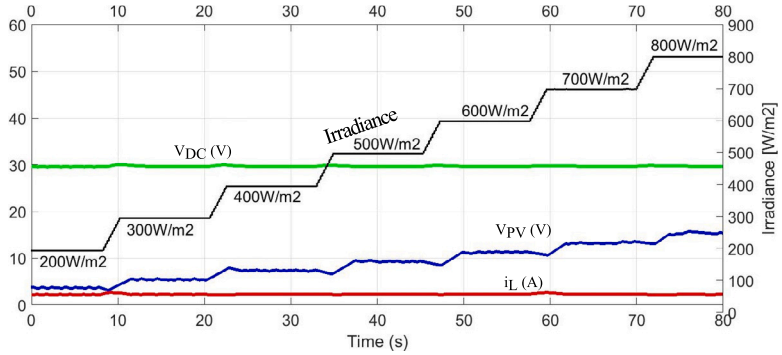

Fig. 12. Irradiation variation test for SMPIC.

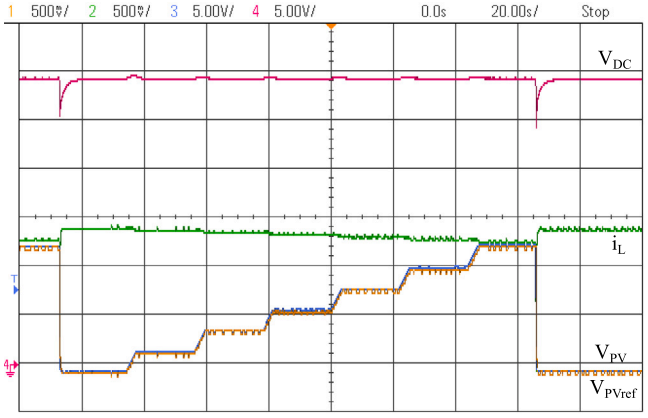

Fig. 13. Irradiance — fast variance under SMC control.

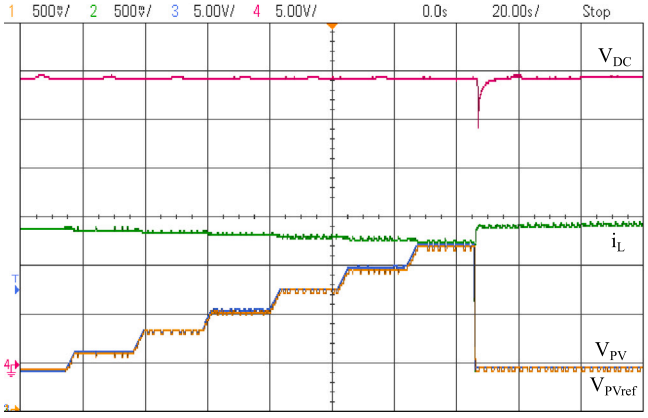

Fig. 14. Irradiance — fast variance under SMPI control.

those aforementioned disadvantages are minimized. The plant is connected to the cloud server by TCP/IP. The server runs the GA algorithm that allows to tune the SMC gains. The optimization process is slow and some spikes could happen, so once the parameters are found, system can run in normal mode. Optimization mode can be active anytime when needed.

As shown in Section 4, this work shows a better performance for the tunned controllers than previous SMC and SMPIC boost converters for both current control loop and voltage control loops, as seen in voltage steps settling times and overshoot comparison. In addition, the previous works were simulated employing w-PSO to optimize its parameters before being carried over to prototype, this new proposed versatile technique has better results due to the possibility of the optimization be executed in runtime. Even in

irradiation variation, the controllers present a satisfactory performance, with boosted output stability, low steady state error and a faster response.

The implementation of this scheme is possible due to the DSP capability to run real-time control and perform internet communication in parallel. The IoT conception brought the possibility to monitor, diagnose and even calibrate the system.

Declaration of competing interest

The authors declare that they have no known competing financial interests or personal relationships that could have appeared to influence the work reported in this paper.

Data availability

Data will be made available on request.

Acknowledgment

CNPq - *Conselho Nacional de Desenvolvimento Científico e Tecnológico* grant ID: 407867/2022-8 and *FAPESP - Fundação de Amparo à Pesquisa do Estado de São Paulo* grant ID: 2022/00323-3.

References

[1] Karami N, Moubayed N, Outbib R. General review and classification of different MPPT techniques. Renew Sustain Energy Rev 2017;68:1–18. http://dx.doi.org/10.1016/j.rser.2016.09.132, URL https://www.sciencedirect.com/science/article/pii/S1364032116306438.
[2] Mirzal A, Yoshii S, Furukawa M. PID parameters optimization by using genetic algorithm: A study on time-delay systems. ISTECS J 2006;8:34–43.
[3] Fernandes D, Almeida R, Guedes T, Sguarezi Filho A, Costa F. State feedback control for DC-photovoltaic systems. Electr Power Syst Res 2017;143:794–801. http://dx.doi.org/10.1016/j.epsr.2016.08.037.
[4] Ilyas A, Khan MR, Ayyub M. FPGA based real-time implementation of fuzzy logic controller for maximum power point tracking of solar photovoltaic system. Optik 2020;213:164668. http://dx.doi.org/10.1016/j.ijleo.2020.164668, URL https://www.sciencedirect.com/science/article/pii/S0030402620305027.
[5] Njomo AFT, Sonfack LL, Douanla RM, Kenne G. Nonlinear neuro-adaptive control for MPPT applied to photovoltaic systems. J Control Autom Electr Syst 2021;32(3):693–702. http://dx.doi.org/10.1007/s40313-021-00691-3.
[6] Bellinaso LV, Figueira HH, Basquera MF, Vieira RP, Gründling HA, Michels L. Cascade control with adaptive voltage controller applied to photovoltaic boost converters. IEEE Trans Ind Appl 2019;55(2):1903–12. http://dx.doi.org/10.1109/TIA.2018.2884904.
[7] Cunha R, Inomoto R, Altuna J, Costa F, Di Santo S, Sguarezi Filho A. Constant switching frequency finite control set model predictive control applied to the boost converter of a photovoltaic system. Sol Energy 2019;189:57–66. http://dx.doi.org/10.1016/j.solener.2019.07.021, URL https://www.sciencedirect.com/science/article/pii/S0038092X19306838.
[8] Filho AJS, Inomoto RS, Rodrigues LL, Cunha RBA, Vilcanqui OAC. Predictive control applied to a boost converter of a photovoltaic system. J Control Autom Electr Syst 2021. http://dx.doi.org/10.1007/s40313-021-00796-9.
[9] Priyadarshi N, Padmanaban S, Bhaskar Ranjana M, Azam F, Taha I, Mousa Hussien MG. An adaptive TS-fuzzy model based RBF neural network learning for grid integrated photovoltaic applications. Renew Power Gener IET 2022;16. http://dx.doi.org/10.1049/rpg2.12505.
[10] Vargas Gil GM, Lima Rodrigues L, Inomoto RS, Sguarezi AJ, Machado Monaro R. Weighted-PSO applied to tune sliding mode plus PI controller applied to a boost converter in a PV system. Energies 2019;12(5). http://dx.doi.org/10.3390/en12050864, URL https://www.mdpi.com/1996-1073/12/5/864.
[11] Inomoto RS, Monteiro JRBA, Sguarezi Filho AJ. Boost converter control of PV system using sliding mode control with integrative sliding surface. IEEE J Emerg Sel Top Power Electron 2022. http://dx.doi.org/10.1109/JESTPE.2022.3158247, 1–1.
[12] Bounar N, Labdai S, Boulkroune A. PSO–GSA based fuzzy sliding mode controller for DFIG-based wind turbine. ISA Trans 2019;85:177–88. http://dx.doi.org/10.1016/j.isatra.2018.10.020, URL https://www.sciencedirect.com/science/article/pii/S0019057818303999.
[13] Holland JH. Adaptation in natural and artificial systems: an introductory analysis with applications to biology, control, and artificial intelligence. MIT Press; 1992.
[14] Benhlima S, Chaymaa L, Bekri A. Genetic algorithm based approach for autonomous mobile robot path planning. Procedia Comput Sci 2018;127. http://dx.doi.org/10.1016/j.procs.2018.01.113.
[15] Wang Q, Xi H, Deng F, Cheng M, Buja G. Design and analysis of genetic algorithm and BP neural network based PID control for boost converter applied in renewable power generations. IET Renew Power Gener 2022;16(7):1336–44. http://dx.doi.org/10.1049/rpg2.12320, arXiv:https://ietresearch.onlinelibrary.wiley.com/doi/pdf/10.1049/rpg2.12320. URL https://ietresearch.onlinelibrary.wiley.com/doi/abs/10.1049/rpg2.12320.
[16] Sivamani D, Shyam D, Ali AN, Premkumar K, Narendiran S, Alexander SA. Solar powered battery charging system using optimized PI controller for buck boost converter. IOP Conf Ser: Mater Sci Eng 2021;1055(1):012151. http://dx.doi.org/10.1088/1757-899x/1055/1/012151.
[17] Silverio M, Renukappa S, Suresh S. What is a smart device? - A conceptualisation within the paradigm of the internet of things. Vis Eng 2018;6. http://dx.doi.org/10.1186/s40327-018-0063-8.
[18] Potter C, Hancke G, Silva B. Machine-to-machine: Possible applications in industrial networks. In: 2013 IEEE international conference on industrial technology. ICIT, 2013, p. 1321–6. http://dx.doi.org/10.1109/ICIT.2013.6505864.
[19] Rouibah N, Barazane L, Benghanem M, Mellit A. IoT-based low-cost prototype for online monitoring of maximum output power of domestic photovoltaic systems. ETRI J 2021;43(3):459–70. http://dx.doi.org/10.4218/etrij.2019-0537, arXiv:https://onlinelibrary.wiley.com/doi/pdf/10.4218/etrij.2019-0537. URL https://onlinelibrary.wiley.com/doi/abs/10.4218/etrij.2019-0537.
[20] J B, Moses M. IOT based augmented perturb-and-observe soft switching boost converters for photovoltaic power systems in smart cities. Wirel Pers Commun 2018;102:2619–41. http://dx.doi.org/10.1007/s11277-018-5280-x.
[21] Rouibah N, Barazane L, Mellit A, Hajji B, Rabhi A. A low-cost monitoring system for maximum power point of a photovoltaic system using IoT technique. In: 2019 international conference on wireless technologies, embedded and intelligent systems. WITS, 2019, p. 1–5. http://dx.doi.org/10.1109/WITS.2019.8723724.
[22] Rokonuzzaman M, Shakeri M, Hamid FA, Mishu MK, Pasupuleti J, Rahman KS, Tiong SK, Amin N. IoT-enabled high efficiency smart solar charge controller with maximum power point tracking—Design, hardware implementation and performance testing. Electronics 2020;9(8). http://dx.doi.org/10.3390/electronics9081267, URL https://www.mdpi.com/2079-9292/9/8/1267.

[23] Habib M, Gram A, Harrag A, Wang Q. Optimized management of reactive power reserves of transmission grid-connected photovoltaic plants driven by an IoT solution. Int J Electr Power Energy Syst 2022;143:108455. http://dx.doi.org/10.1016/j.ijepes.2022.108455, URL https://www.sciencedirect.com/science/article/pii/S0142061522004641.
[24] Erickson RW, Maksimovic D. Fundamentals of power electronics. Kluwer Academic Publishers; 2004.
[25] Mohan N, Undeland TM, Robbins WP. Power electornics - converters, applications, and design. John & Sons, Inc; 1995.
[26] Villalva M, de Siqueira T, Ruppert E. Voltage regulation of photovoltaic arrays: small-signal analysis and control design. IET Power Electron 2010;3:869–80. http://dx.doi.org/10.1049/iet-pel.2008.0344.
[27] Rezaei MM, Asadi H. A modified perturb-and-observe-based maximum power point tracking technique for photovoltaic energy conversion systems. J Control Autom Electr Syst 2019;30. http://dx.doi.org/10.1007/s40313-019-00495-6.
[28] Trindade FS, Filho AJS, Jacomini RV, Ruppert E. Experimental results of sliding-mode power control for doubly-fed induction generator. In: 2013 Brazilian power electronics conference. 2013, p. 686–91. http://dx.doi.org/10.1109/COBEP.2013.6785189.
[29] Monteiro JRBA, Oliveira CMR, Almeida TEP, Cezare MJ. Pseudo sliding mode control with integrative action applied to brushless DC motor speed control. In: 2015 IEEE 13th Brazilian power electronics conference and 1st southern power electronics conference. COBEP/SPEC, 2015, p. 1–6. http://dx.doi.org/10.1109/COBEP.2015.7420076.
[30] Aghaei M, Esksndari A, Reinders A. Autonomous monitoring and analysis of PV systems by unmanned aerial vehicles, internet of things and big data analytics. In: Conference: 37th European photovoltaic solar energy conference and exhibition. 2020, http://dx.doi.org/10.4229/EUPVSEC20202020-5DO.3.5.
[31] Shukla A, Pandey HM, Mehrotra D. Comparative review of selection techniques in genetic algorithm. In: 2015 international conference on futuristic trends on computational analysis and knowledge management. ABLAZE, 2015, p. 515–9. http://dx.doi.org/10.1109/ABLAZE.2015.7154916.
[32] Zhong J, Hu X, Zhang J, Gu M. Comparison of performance between different selection strategies on simple genetic algorithms. In: International conference on computational intelligence for modelling, control and automation and international conference on intelligent agents, web technologies and internet commerce. CIMCA-iAWTIC'06, Vol. 2, 2005, p. 1115–21. http://dx.doi.org/10.1109/CIMCA.2005.1631619.
[33] Lata S, Yadav S, Sohal A. Comparative study of different selection techniques in genetic algorithm. Internat J Engrg Sci 2017.
[34] IEEE standard for floating-point arithmetic. IEEE std 754-2019 (revision of IEEE 754-2008), 2019, p. 1–84. http://dx.doi.org/10.1109/IEEESTD.2019.8766229.
[35] Whitley D. A genetic algorithm tutorial. Stat Comput 1998;4. http://dx.doi.org/10.1007/BF00175354.
[36] Bhardwaj M, Subharmanya B. PV inverter design using solar explorer kit. URL http://www.ti.com/lit/an/sprabr4a/sprabr4a.pdf.
[37] Meddour S, Rahem D, Wira P, Laib H, Cherif AY, Chtouki I. Design and implementation of an improved metaheuristic algorithm for maximum power point tracking algorithm based on a PV emulator and a double-stage grid-connected system. Eur J Electr Eng/Rev Int Génie Electr 2022;24(3).